

Estimation of general Hamiltonian parameters via controlled energy measurements

Luigi Seveso^{1,*} and Matteo G. A. Paris^{1,2,†}

¹*Quantum Technology Lab, Dipartimento di Fisica dell'Università degli Studi di Milano, I-20133 Milano, Italia*

²*Istituto Nazionale di Fisica Nucleare, Sezione di Milano, I-20133 Milano, Italy*

The quantum Cramér-Rao theorem states that the quantum Fisher information (QFI) bounds the best achievable precision in the estimation of a quantum parameter ξ . This is true, however, under the assumption that the measurement employed to extract information on ξ are regular, i.e. neither its sample space nor its positive-operator valued elements depend on the (true) value of the parameter. A better performance may be achieved by relaxing this assumption. In the case of a general Hamiltonian parameter, i.e. when the parameter enters the system's Hamiltonian in a non-linear way (making the energy eigenstates and eigenvalues ξ -dependent), a family of non-regular measurements, referred to as controlled energy measurements, is naturally available. We perform an analytic optimization of their performance, which enables us to compare the optimal controlled energy measurement with the optimal Braunstein-Caves measurement based on the symmetric logarithmic derivative. As the former may outperform the latter, the ultimate quantum bounds for general Hamiltonian parameters are different than those for phase (shift) parameters. We also discuss in detail a realistic implementation of controlled energy measurements based on the quantum phase estimation algorithm and work out a variety of examples to illustrate our results.

I. INTRODUCTION

Quantum parameter estimation studies the statistical inference of an unknown parameter from the empirical data generated by a quantum system. The possible states of the system are described by a statistical model, i.e. a family of density operators ρ_ξ , parametrized by ξ . An estimate of ξ is obtained by performing a measurement on the system and then processing the outcomes via a point estimator $\hat{\xi}$ [1–4]. The overall task of parameter estimation is to optimize over the choice of both the measurement and the estimator, in order to minimize, on average, a given loss function.

The parameter to be estimated usually corresponds to a physical quantity which is not directly measurable. Quantum estimation is therefore particularly relevant to the field of quantum technologies, since knowledge of inaccessible parameters is often required for quantum control. Following the pioneering works by Helstrom [5] and Holevo [6], it was discovered that estimation strategies exploiting quantum effects (such as squeezing [7] and entanglement [8–10]) can outperform any classical strategy using the same resources (at least under ideal conditions [11–13]). Quantum parameter estimation has thus become the theoretical foundation of quantum metrology [14–17], besides being linked to branches of pure mathematics, from statistics to information geometry [18–20].

An important class of estimation problems is concerned with parameters characterizing the Hamiltonian H_ξ of a closed quantum system. These problems are referred to as Hamiltonian estimation problems, and the corresponding parameters ξ as Hamiltonian parameters. One further distinguishes between phase (or shift) parameters and general parameters. In the former case, the parameter ξ appears as an overall multiplicative constant, i.e. $H_\xi = \xi G$, with G being the generator of the system's dynamics. The phase estimation problem is well studied, both in the decoherence-free

and noisy scenarios, with applications to optical interferometry, imaging and atomic spectroscopy [21–31]. The case of a general Hamiltonian parameter, i.e. when both the eigenvalues and the eigenvectors of H_ξ depend on ξ , has been investigated only more recently [32–35].

In a Hamiltonian estimation problem, the system is initialized in the state ρ_0 , the parameter is encoded through the unitary channel generated by H_ξ and, finally, a measurement \mathcal{M} is implemented. The outcomes of N independent repetitions of the protocol are fed into an estimator $\hat{\xi}$, yielding an estimate of the parameter. If the estimator is unbiased and the loss function is the estimator's variance, then the performance of any estimation strategy is limited by the Cramér-Rao bound

$$\text{Var}(\hat{\xi}) \geq [N\mathcal{F}_\xi(\rho_0, \mathcal{M})]^{-1},$$

where \mathcal{F}_ξ denotes the Fisher information (FI) [36–38]. The maximum of the FI over all possible initial preparations ρ_0 and measurements \mathcal{M} is, by definition, the channel quantum Fisher information (CQFI) [39]. The corresponding quantum Cramér-Rao bound

$$\text{Var}(\hat{\xi}) \geq [N\mathcal{F}_\xi^{(Q,C)}]^{-1}$$

may be saturated by preparing the system in the optimal initial state, implementing the optimal measurement and processing the outcomes via an efficient estimator [40]. The quantum Cramér-Rao is usually regarded as the ultimate quantum limit to precision, at least in the single parameter scenario [41], to which we will restrict our attention.

As argued in Ref. [34], in the estimation of a general Hamiltonian parameter, an enhanced precision limit is achievable. In a nutshell, the argument is as follows. The CQFI is the maximum FI, optimized over all initial preparations ρ_0 and over all *regular* measurements, i.e. measurements that are independent of the (unknown) true value of the parameter. The requirement that the measurement is parameter-independent is a natural assumption, analogous to the condition, for a classical statistical model p_ξ , that the support $\text{supp}(p_\xi)$ is indepen-

* luigi.seveso@unimi.it

† matteo.paris@fisica.unimi.it

dent of ξ , which is a fundamental prerequisite for the Cramér-Rao bound to hold. Nonetheless, non-regular classical models have also been considered in the literature [42–47]. In such cases, an estimator performing better than predicted by the Cramér-Rao bound may exist [48]. Likewise, a quantum estimation strategy is referred to as regular if both the sample space \mathcal{X} of possible outcomes and the POVM elements $\{\Pi_x\}_{x \in \mathcal{X}}$ are parameter-independent. In the context of a general Hamiltonian estimation problem, an energy measurement (i.e. a projective measurement onto the eigenstates of the Hamiltonian H_ξ) is non-regular. In fact, both the outcomes of the measurement (the eigenvalues of H_ξ) and the detection operators (the projectors over its eigenstates) depend on ξ . The assessment of the best achievable precision becomes highly non-trivial in this case. In particular, the ultimate bound is no longer given by the CQFI.

Here, we further advance the analysis carried out in Ref. [34], specializing it to a class of non-regular measurements (referred to as *controlled energy measurements*) that arise in the estimation of a general Hamiltonian parameter. Having circumscribed the set of non-regular strategies under considerations, one is confronted with task of maximizing the precision over such a set. This is analogous to the introduction of the quantum Fisher information by a process of optimization over the set of regular measurements. One of the main results of the present manuscript is an analytic bound (which can be saturated under suitable conditions) to the best precision achievable via controlled energy measurements. We also discuss their experimental feasibility and propose a realistic implementation based on the quantum phase estimation algorithm. Finally, a collection of examples is employed to illustrate our results and emphasize that an enhancement (with respect to regular estimation strategies) can often be realized in practice.

The rest of the manuscript is organized as follows. Section II contains a basic review of quantum parameter estimation theory. In Section III, we introduce the family of controlled energy measurements, together with the information quantity \mathcal{G}_ξ , which quantifies the maximum extractable information in our setting. In Section IV, an upper-bound to \mathcal{G}_ξ is derived, which is shown in Section V to be tight for a large class of Hamiltonian problems. In Section VI we illustrate the relevance of our results to quantum metrology applications, showing how to perform a controlled energy measurement on a generic physical system. Finally, in Section VII, a collection of examples is worked out. Section VIII closes the paper with some concluding remarks.

II. PRELIMINARIES

We restrict ourselves to the case of a finite-dimensional quantum system with Hilbert space $\mathcal{H} = \mathbb{C}^d$. The generator of the system's noiseless evolution is its Hamiltonian $H_\xi \in \text{Her}_d(\mathbb{C})$, where $\text{Her}_d(\mathbb{C})$ is the set of $d \times d$ Hermitian matrices. The Hamiltonian H_ξ depends generically on a parameter ξ , taking values in a parameter space $\Xi \subset \mathbb{R}$. Given a matrix $M \in \text{Her}_d(\mathbb{C})$, the following

standard notation is employed: M has d real eigenvalues $\text{spec}(M) = \{\lambda_1(M), \dots, \lambda_d(M)\}$, ordered decreasingly, i.e. $\lambda_1(M) \geq \dots \geq \lambda_d(M)$. The spectral gap $\sigma(M)$ is defined as the difference between its extremal eigenvalues, i.e. $\sigma(M) := \lambda_d(M) - \lambda_1(M)$.

The computational basis of \mathcal{H} is denoted by $|j\rangle$, with $j \in \{0, \dots, d-1\}$, while the basis made up of the eigenstates of the Hamiltonian is denoted by $|E_{j,\xi}\rangle$; the subscript emphasizes that the energy eigenstates are ξ -dependent. By definition, $H_\xi |E_{j,\xi}\rangle = E_{j,\xi} |E_{j,\xi}\rangle$, where $E_{j,\xi} := \lambda_{d-j}(H)$ are the eigenvalues of H_ξ . For simplicity, the spectrum of H_ξ is assumed to be non-degenerate; however, everything that follows holds more generally also in the presence of degeneracies, with minor adaptations. For future convenience, we denote the projectors onto the computational basis (*resp.*, the energy eigenbasis) by $P_j := |j\rangle\langle j|$ (*resp.*, $P_{E_{j,\xi}} := |E_{j,\xi}\rangle\langle E_{j,\xi}|$). The two basis are mapped one into the other by a suitable unitary similarity transformation S_ξ , i.e. $|j\rangle = S_\xi |E_{j,\xi}\rangle$. Explicitly, the matrix elements of S_ξ can be computed as $\langle j|S_\xi|k\rangle = \langle E_{j,\xi}|k\rangle$. Notice that S_ξ reduces H_ξ to diagonal form, i.e. $S_\xi H_\xi S_\xi^\dagger = \text{diag}(E_{0,\xi}, \dots, E_{d-1,\xi})$, and that the matrix S_ξ is ξ -dependent for a general Hamiltonian parameter.

A typical quantum estimation strategy consists of the following steps: the system is initialized in the state ρ_0 ; then, the unitary map generated by H_ξ encodes the parameter into the model $\rho_\xi := U_t \rho_0 U_t^\dagger$, with $U_t := \exp(-itH_\xi)$ and t the interrogation time; finally, a measurement \mathcal{M} is performed. A measurement is defined in terms of its positive-operator valued measure (POVM) $\{\Pi_x\}_{x \in \mathcal{X}}$. Each Π_x is a positive Hermitian operator, satisfying the completeness property $\sum_{x \in \mathcal{X}} \Pi_x = \mathbb{I}_d$, where \mathbb{I}_d is the $d \times d$ identity matrix and the sample space $\mathcal{X} \subset \mathbb{R}$ is assumed to be a finite set. If both the sample space \mathcal{X} and the POVM elements Π_x do not depend on ξ , then the estimation strategy, as well as the measurement \mathcal{M} , are called *regular*; the family of all possible regular measurements is denoted by \mathcal{R} . Any given outcome $x \in \mathcal{X}$ is obtained with corresponding probability $p_{x,\xi} = \text{tr}[\rho_\xi \Pi_x]$. Over N repetitions of the protocol, one obtains a sample $\mathbf{x} \in \mathcal{X}^{\times N}$, which is processed via an estimator $\hat{\xi} : \mathcal{X}^{\times N} \rightarrow \xi$, yielding an estimate $\hat{\xi}(\mathbf{x})$ of the parameter.

Consider the set of all possible estimation strategies, with ρ_0 and \mathcal{M} fixed, $\mathcal{M} \in \mathcal{R}$ and $\hat{\xi}$ an unbiased estimator, i.e.

$$\mathbb{E}(\hat{\xi}) := \sum_{\mathbf{x} \in \mathcal{X}^{\times N}} p_{\mathbf{x},\xi} \hat{\xi}(\mathbf{x}) = \xi, \quad \forall \xi \in \Xi. \quad (1)$$

where $p_{\mathbf{x},\xi}$ is the joint probability distribution of the N outcomes. Then, if the variance $\text{Var}(\hat{\xi})$ is taken as the loss function, the Cramér-Rao theorem [36–38] states that the best performing strategy, optimized over the choice of the estimator, saturates the inequality

$$\text{Var}(\hat{\xi}) \geq \frac{1}{N \cdot \mathcal{F}_\xi(\rho_0, \mathcal{M})}. \quad (2)$$

The FI $\mathcal{F}_\xi(\rho_0, \mathcal{M})$ is defined as follows

$$\begin{aligned} \mathcal{F}_\xi(\rho_0, \mathcal{M}) &:= \sum_{x \in \mathcal{X}} p_{x, \xi} (\partial_\xi \ln p_{x, \xi})^2 \\ &= \sum_{x \in \mathcal{X}} \text{tr}[\rho_\xi \Pi_x] (\partial_\xi \ln \text{tr}[\rho_\xi \Pi_x])^2. \end{aligned} \quad (3)$$

We refer the interested reader to [1–3] for precise conditions under which (2) holds and can be achieved.

The next step is to optimize over the choice of the measurement \mathcal{M} . One introduces the QFI $\mathcal{F}_\xi^{(Q)}(\rho_0)$ as

$$\mathcal{F}_\xi^{(Q)}(\rho_0) = \max_{\mathcal{M} \in \mathcal{R}} \mathcal{F}_\xi(\rho_0, \mathcal{M}). \quad (4)$$

Braunstein and Caves [39, 49] have proved that the QFI coincides with the least monotone quantum Riemannian metric in the Petz classification [50], which is the one based on the symmetric logarithmic derivative (SLD) [51], so that

$$\mathcal{F}_\xi^{(Q)}(\rho_0) = \text{tr}[\rho_\xi L_{\rho, \xi}^2], \quad \partial_\xi \rho_\xi = \frac{1}{2} \{\rho_\xi, L_{\rho, \xi}\}, \quad (5)$$

where $L_{\rho, \xi}$ is the SLD of ρ_ξ . Therefore, the best performing strategy, optimized over the set of all (regular) measurements and unbiased estimators, for fixed initial preparation, saturates the inequality

$$\text{Var}(\hat{\xi}) \geq \frac{1}{N \cdot \mathcal{F}_\xi^{(Q)}(\rho_0)}. \quad (6)$$

Implementing the optimal Braunstein-Caves strategy requires performing a projective measurement over the eigenstates of $L_{\rho, \xi}$ and post-processing the outcomes via an efficient estimator [52]. For pure models, i.e. $\rho_0 = |\psi_0\rangle\langle\psi_0|$ and thus $\rho_\xi = |\psi_\xi\rangle\langle\psi_\xi|$ with $|\psi_\xi\rangle = U_t |\psi_0\rangle$, the QFI can be computed explicitly [17] as

$$\begin{aligned} \mathcal{F}_\xi^{(Q)}(\rho_0) &= 4 \text{Var}_{|\psi_\xi\rangle} \mathfrak{g}_{U, \xi} \\ &= 4 \left[\langle \psi_\xi | \mathfrak{g}_{U, \xi}^2 | \psi_\xi \rangle - \langle \psi_\xi | \mathfrak{g}_{U, \xi} | \psi_\xi \rangle^2 \right], \end{aligned} \quad (7)$$

where

$$\mathfrak{g}_{U, \xi} := i \partial_\xi U_t U_t^\dagger \quad (8)$$

is the local generator of U_t with respect to the parameter ξ .

The final step is to optimize over the initial preparation ρ_0 . The channel quantum Fisher information (CQFI) is defined as

$$\mathcal{F}_\xi^{(Q, C)} = \max_{\rho_0} \mathcal{F}_\xi^{(Q)}(\rho_0). \quad (9)$$

The QFI is a convex functional of the initial preparation, so that the maximum of Eq. (9) can be looked for on the set of pure states $\rho_0 = |\psi_0\rangle\langle\psi_0|$. Since

$$\mathcal{F}_\xi^{(Q)}(|\psi_0\rangle\langle\psi_0|) = 4 \text{Var}_{|\psi_0\rangle} U_t^\dagger \mathfrak{g}_{U, \xi} U_t, \quad (10)$$

and moreover, by Popoviciu's inequality [53], the variance of

a random variable X , with maximum value x_M and minimum value x_m , is upper-bounded by $(x_M - x_m)^2/4$, it follows that

$$\begin{aligned} \mathcal{F}_\xi^{(Q, C)} &\leq [\lambda_1(U_t^\dagger \mathfrak{g}_{U, \xi} U_t) - \lambda_d(U_t^\dagger \mathfrak{g}_{U, \xi} U_t)]^2 \\ &= [\lambda_1(\mathfrak{g}_{U, \xi}) - \lambda_d(\mathfrak{g}_{U, \xi})]^2. \end{aligned} \quad (11)$$

Since a balanced superposition of the extremal eigenvectors of $\mathfrak{g}_{U, \xi}$ achieves the RHS of the previous inequality, the inequality is tight and thus the CQFI is related to the spectral gap of the local generator $\mathfrak{g}_{U, \xi}$ via

$$\mathcal{F}_\xi^{(Q, C)} = (\sigma[\mathfrak{g}_{U, \xi}])^2. \quad (12)$$

Eq. (12) is the maximum information which can be extracted on ξ via any regular quantum estimation strategy.

III. NON-REGULAR ESTIMATION OF HAMILTONIAN PARAMETERS

A non-regular measurement depends intrinsically on the true value of the parameter, either via its sample space \mathcal{X}_ξ , or its POVM elements $\Pi_{x, \xi}$ (or both). The latter circumstance is specific to quantum parameter estimation, whereas the former has a classical analogue when the support of the statistical model p_ξ is parameter-dependent. In such cases, it often happens that there exists a locally unbiased estimator with vanishing variance [48], so that the achievable precision is formally unbounded.

As argued before, in the estimation of a general Hamiltonian parameter, a projective measurement of H_ξ is non-regular, since either the eigenvalues, or the eigenstates of H_ξ , or both, depend on ξ . The first scenario would lead to a parameter-dependent sample space, the same situation one encounters in non-regular classical estimation. Assessing the performance of different strategies becomes a difficult matter; moreover, there is often no non-trivial lower bound to the variance of an unbiased estimator. In the rest of the manuscript, we will thus focus exclusively on the second case. That is, we are going to assume that either only the eigenvectors of H_ξ depend on ξ , or that a data post-processing takes place after the energy measurement, which maps the original, parameter-dependent sample-space to a fixed, parameter-independent one. An energy measurement is thus modified by introducing a 1-1 map $\pi : \mathcal{X}_\xi \rightarrow \mathcal{Y}$, with \mathcal{X}_ξ consisting of the eigenvalues of H_ξ , so that the sample space of the measurement is $\pi(\mathcal{X}_\xi)$, while its POVM elements are unchanged. The estimation strategy is still non-regular, but the possibility of pathological estimators with vanishing variance is excluded and the FI is again the relevant performance metric.

We now introduce a family of non-regular measurements $\mathcal{M}_{V, \xi}$, which is denoted by \mathcal{E} ; each measurement in \mathcal{E} is labelled by an arbitrary unitary control V . By definition, the measurement $\mathcal{M}_{V, \xi}$ has POVM elements $V^\dagger P_{E_j, \xi} V$. It will be called a controlled energy measurement, since its implementation requires to apply a unitary, parameter-independent control V to the system and thereafter measure its energy.

In the absence of controls, a bare energy measurement

($V = \mathbb{I}_d$) obeys the statistics

$$p_{E_j, \xi} = \text{tr}[\rho_\xi P_{E_j, \xi}] = \langle E_j, \xi | \rho_0 | E_j, \xi \rangle, \quad (13)$$

which does not depend on the interrogation time t . As a consequence, the corresponding FI $\mathcal{F}_\xi(\rho_0, \mathcal{M}_{\mathbb{I}_d, \xi})$ is also independent of t . In contrast, the QFI $\mathcal{F}_\xi^{(Q, C)}(\rho_0)$ grows generically like t^2 [33]. If, however, a control is applied before the measurement, then the FI $\mathcal{F}_\xi(\rho_0, \mathcal{M}_{V, \xi})$ is again allowed to grow quadratically with t . This argument shows the metrological usefulness of controls in conjunction with an energy measurement.

Finally, in analogy with the CQFI, we define the following information quantity

$$\mathcal{G}_\xi = \max_{\rho_0} \max_{\mathcal{M}_{V, \xi} \in \mathcal{E}} \mathcal{F}_\xi(\rho_0, \mathcal{M}_{V, \xi}). \quad (14)$$

It represents the maximum extractable information on a general Hamiltonian parameter via controlled energy measurements, optimized over the set of initial preparations ρ_0 and unitary controls.

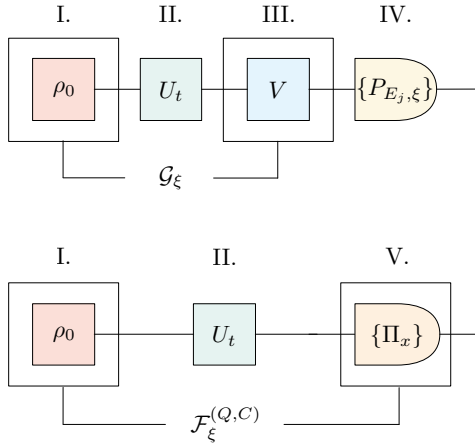


FIG. 1. Comparison between an estimation strategy based on a controlled energy measurement (*upper scheme*) and one based on a regular measurement (*lower scheme*). In the first case, the optimal performance is quantified by \mathcal{G}_ξ , which is optimized over the preparation and control steps; in the second, it is quantified by the CQFI $\mathcal{F}_\xi^{(Q, C)}$, which instead is optimized over all initial preparations and (regular) measurements. The different stages of the schemes are denoted as follows: I. \rightarrow preparation, II. \rightarrow encoding, III. \rightarrow control, IV. \rightarrow energy measurement and V. \rightarrow regular measurement.

We summarize the preceding discussion via the following two definitions (see also Fig. 1):

DEFINITION 1. Given a quantum system with Hamiltonian H_ξ and unknown parameter $\xi \in \Xi$, a controlled energy measurement, denoted by $\mathcal{M}_{V, \xi}$, is defined through its POVM elements $V^\dagger P_{E_j, \xi} V$, where V is a unitary control and $P_{E_j, \xi}$ is the projector over the j^{th} energy eigenstate.

DEFINITION 2. The information quantity \mathcal{G}_ξ is the maximum Fisher information $\mathcal{F}_\xi(\rho_0, \mathcal{M}_{V, \xi})$, optimized over both

the set of initial preparations ρ_0 and controlled energy measurements $\mathcal{M}_{V, \xi}$.

Let us remark that the performance of an estimation strategy making use of a controlled energy measurement is not necessarily bounded by the CQFI of Eq. (12), i.e. \mathcal{G}_ξ may exceed $\mathcal{F}_\xi^{(Q, C)}$. However, computing \mathcal{G}_ξ directly from its definition (14) is non-trivial. In the following, a closed-form expression for \mathcal{G}_ξ (similar to Eq. (12) for $\mathcal{F}_\xi^{(Q, C)}$) is derived under the hypothesis that the Hamiltonian H_ξ satisfies a rather general mathematical condition. For Hamiltonians not satisfying such condition, it only provides an upper-bound to \mathcal{G}_ξ , which is not necessarily tight. With the help of this result, we will be able to compare regular estimation strategies with non-regular ones based on controlled energy measurements.

IV. BOUNDING \mathcal{G}_ξ

Consider a non-regular estimation strategy based on the controlled energy measurement $\mathcal{M}_{V, \xi}$. The probability distribution of the measurement outcomes is given by

$$\begin{aligned} p_{\pi(E_j, \xi), \xi} &= \text{tr}[\rho_\xi V^\dagger P_{E_j, \xi} V] \\ &= \text{tr}[(S_\xi V U_t) \rho_0 (S_\xi V U_t)^\dagger P_j] \\ &= \text{tr}[\mathcal{U}_V \rho_0 \mathcal{U}_V^\dagger P_j], \end{aligned} \quad (15)$$

where all dependence on ξ has been collected in the unitary matrix $\mathcal{U}_V := S_\xi V U_t$. We define the statistical model $\rho_{V, \xi} := \mathcal{U}_V \rho_0 \mathcal{U}_V^\dagger$ as the model which one would obtain if the parameter were encoded on the initial preparation ρ_0 through \mathcal{U}_V , instead of U_t ; it is referred to as the auxiliary statistical model associated to the physical model ρ_ξ . It follows from Eq. (15) that the FI $\mathcal{F}_\xi(\rho_0, \mathcal{M}_{V, \xi})$, for the non-regular estimation strategy we are considering, is formally equal to the FI corresponding to a projective measurement in the computational basis on the auxiliary model, i.e.

$$\mathcal{F}_\xi(\rho_0, \mathcal{M}_{V, \xi}) = \sum_{j=0}^{d-1} \frac{(\partial_\xi \text{tr}[\rho_{V, \xi} P_j])^2}{\text{tr}[\rho_{V, \xi} P_j]}. \quad (16)$$

Following Braunstein and Caves [39], the Fisher information (16) can be majorized as follows. After expressing the derivative at the numerator as $\partial_\xi \rho_{V, \xi} = \{\rho_{V, \xi}, L_{\rho_{V, \xi}}\}/2$, where $L_{\rho_{V, \xi}}$ is the SLD of the auxiliary model, one obtains

$$\begin{aligned} \mathcal{F}_\xi(\rho_0, \mathcal{M}_{V, \xi}) &= \frac{1}{2} \sum_{j=0}^{d-1} \frac{(\text{tr}[\{\rho_{V, \xi}, L_{\rho_{V, \xi}}\} P_j])^2}{\text{tr}[\rho_{V, \xi} P_j]} \\ &= \sum_{j=0}^{d-1} \frac{\Re^2(\text{tr}[\rho_{V, \xi} L_{\rho_{V, \xi}} P_j])}{\text{tr}[\rho_{V, \xi} P_j]} \\ &\leq \sum_{j=0}^{d-1} \frac{|\text{tr}[\rho_{V, \xi} L_{\rho_{V, \xi}} P_j]|^2}{\text{tr}[\rho_{V, \xi} P_j]}, \end{aligned} \quad (17)$$

where use was made of the triangular inequality $\Re z \leq |z|$, $\forall z \in \mathbb{C}$.

Next, by the Cauchy-Schwarz inequality, the numerator can be bounded as follows,

$$|\text{tr}[\rho_{V,\xi} L_{\rho_{V,\xi}} P_j]|^2 \leq \text{tr}[L_{\rho_{V,\xi}} \rho_{V,\xi} L_{\rho_{V,\xi}} P_j] \text{tr}[\rho_{V,\xi} P_j]. \quad (18)$$

Therefore,

$$\begin{aligned} \mathcal{F}_\xi(\rho_0, \mathcal{M}_{V,\xi}) &\leq \sum_{j=0}^{d-1} \text{tr}[L_{\rho_{V,\xi}} \rho_{V,\xi} L_{\rho_{V,\xi}} P_j] \\ &= \text{tr}[\rho_{V,\xi} (L_{\rho_{V,\xi}})^2]. \end{aligned} \quad (19)$$

Taking the maximum over the initial preparation,

$$\max_{\rho_0} \mathcal{F}_\xi(\rho_0, \mathcal{M}_{V,\xi}) \leq \max_{\rho_0} \text{tr}[\rho_{V,\xi} (L_{\rho_{V,\xi}})^2]. \quad (20)$$

By convexity, the maximum of the expression on the RHS is achieved for a pure initial preparation, i.e. $\rho_0 = |\psi_0\rangle\langle\psi_0|$. On the other hand, for pure initial preparation, one can rewrite it as

$$\text{tr}[\rho_{V,\xi} (L_{\rho_{V,\xi}})^2]_{\rho_0=|\psi_0\rangle\langle\psi_0|} = 4\text{Var}_{|\psi_0\rangle}(\mathcal{U}_V^\dagger \mathfrak{g}_{\mathcal{U}_{V,\xi}} \mathcal{U}_V), \quad (21)$$

where

$$\mathfrak{g}_{\mathcal{U}_{V,\xi}} = \mathfrak{g}_{S,\xi} + (S_\xi V) \mathfrak{g}_{U,\xi} (S_\xi V)^\dagger \quad (22)$$

is the local generator of the unitary encoding \mathcal{U}_V for the auxiliary model. By Popoviciu's inequality, it follows that

$$\max_{\rho_0} \mathcal{F}_\xi(\rho_0, \mathcal{M}_{V,\xi}) \leq (\sigma[\mathfrak{g}_{S,\xi} + (S_\xi V) \mathfrak{g}_{U,\xi} (S_\xi V)^\dagger])^2. \quad (23)$$

Finally, one maximizes over the choice of the unitary control V , i.e.

$$\mathcal{G}_\xi \leq \max_{V \in U(d)} (\sigma[\mathfrak{g}_{S,\xi} + (S_\xi V) \mathfrak{g}_{U,\xi} (S_\xi V)^\dagger])^2. \quad (24)$$

The maximization on the RHS can be carried out explicitly with the help of the following lemma.

LEMMA 1. *Given two Hermitian matrices $M_1, M_2 \in \text{Her}_d(\mathbb{C})$, the maximum spectral gap of the sum of any other two Hermitian matrices \tilde{M}_1, \tilde{M}_2 with the same spectra (i.e. $\text{spec}(M_i) = \text{spec}(\tilde{M}_i)$, $i = 1, 2$) is equal to the sum of the spectral gaps $\sigma(M_1) + \sigma(M_2)$:*

$$\max_{\tilde{M}_1, \tilde{M}_2} \sigma(\tilde{M}_1 + \tilde{M}_2) = \sigma(M_1) + \sigma(M_2). \quad (25)$$

Proof. One may write $\tilde{M}_i = U_i M_i U_i^\dagger$, for suitable unitary matrices U_i , ($i = 1, 2$). Since the spectral gap is invariant under unitary transformations, it follows that

$$\sigma(U_1 M_1 U_1^\dagger + U_2 M_2 U_2^\dagger) = \sigma(M_1 + U M_2 U^\dagger), \quad (26)$$

where $U := U_1^\dagger U_2$. Therefore, we have to prove that

$$\max_{U \in U(d)} \sigma(M_1 + U M_2 U^\dagger) = \sigma(M_1) + \sigma(M_2), \quad (27)$$

By definition, the LHS is equal to

$$\max_{U \in U(d)} [\lambda_1(M_1 + U M_2 U^\dagger) - \lambda_d(M_1 + U M_2 U^\dagger)]. \quad (28)$$

The first term may be bounded as follows,

$$\begin{aligned} \lambda_1(M_1 + U M_2 U^\dagger) &= \max_{|\psi\rangle} \langle\psi|M_1 + U M_2 U^\dagger|\psi\rangle \\ &\leq \max_{|\psi\rangle} \langle\psi|M_1|\psi\rangle + \max_{|\psi\rangle} \langle\psi|U M_2 U^\dagger|\psi\rangle \\ &= \max_{|\psi\rangle} \langle\psi|M_1|\psi\rangle + \max_{|\psi\rangle} \langle\psi|M_2|\psi\rangle \\ &= \lambda_1(M_1) + \lambda_1(M_2). \end{aligned} \quad (29)$$

Similarly, one proves that

$$\lambda_d(M_1 + U M_2 U^\dagger) \geq \lambda_d(M_1) + \lambda_d(M_2). \quad (30)$$

The last two inequalities imply that

$$\sigma(M_1 + U M_2 U^\dagger) \leq \sigma(M_1) + \sigma(M_2). \quad (31)$$

What is left to prove is that the bound is tight. Choose $U = R_1^\dagger R_2$, where R_1 (resp., R_2) is the similarity transformation which diagonalizes M_1 (resp., M_2), with the eigenvalues ordered decreasingly, i.e.

$$\begin{aligned} R_1 M_1 R_1^\dagger &= \text{diag}(\lambda_1(M_1), \dots, \lambda_d(M_1)) := D_1, \\ R_2 M_2 R_2^\dagger &= \text{diag}(\lambda_1(M_2), \dots, \lambda_d(M_2)) := D_2. \end{aligned} \quad (32)$$

Then, for this particular choice of U ,

$$\begin{aligned} \lambda_1(M_1 + U M_2 U^\dagger) &= \lambda_1(R_1 M_1 R_1^\dagger + R_2 M_2 R_2^\dagger) \\ &= \lambda_1(D_1) + \lambda_1(D_2) \\ &= \lambda_1(M_1) + \lambda_1(M_2). \end{aligned} \quad (33)$$

Similarly, one finds that

$$\lambda_d(M_1 + U M_2 U^\dagger) = \lambda_d(M_1) + \lambda_d(M_2). \quad (34)$$

Therefore, the RHS of (31) is achievable. \square

Using the lemma, it follows that the RHS of Eq. (24) is equal to $(\sigma[\mathfrak{g}_{U,\xi}] + \sigma[\mathfrak{g}_{S,\xi}])^2$. We have therefore established the following proposition:

PROPOSITION 1. *Given a finite-dimensional quantum system with Hamiltonian $H_\xi \in \text{Her}_d(\mathbb{C})$ and general parameter $\xi \in \Xi$, the performance of any non-regular estimation strategy based on a controlled energy measurement $\mathcal{M}_{V,\xi}$ is bounded as follows. The maximum extractable information \mathcal{G}_ξ obeys the inequality*

$$\mathcal{G}_\xi \leq (\sigma[\mathfrak{g}_{U,\xi}] + \sigma[\mathfrak{g}_{S,\xi}])^2, \quad (35)$$

where $U_t = \exp(-itH)$ is the unitary encoding, S_ξ is the similarity transformation diagonalizing H_ξ , $\mathfrak{g}_{U,\xi}$ (resp., $\mathfrak{g}_{S,\xi}$) is the generator of U_t (resp., S_ξ), i.e.

$$\mathfrak{g}_{U,\xi} = i\partial_\xi U_t U_t^\dagger, \quad \mathfrak{g}_{S,\xi} = i\partial_\xi S_\xi S_\xi^\dagger, \quad (36)$$

and $\sigma(\cdot)$ denotes the spectral gap.

V. SATURATING THE INEQUALITY IN EQ. (35)

If the eigenvectors of H_ξ do not actually depend on ξ (so that $\partial_\xi S_\xi = 0$) then the set of controlled energy measurements coincides with that of (parameter-independent) projective measurements; since the CQFI is achieved for a projective measurement, it follows that \mathcal{G}_ξ must reduce to the CQFI $\mathcal{F}_\xi^{(Q,C)}$. On the other hand, if $\partial_\xi S_\xi = 0$, then $\sigma(\mathfrak{g}_{S,\xi}) = 0$, so the RHS of inequality (35) is also equal to the CQFI (by comparison with Eq. (9)). Thus, at least in such limiting case, the inequality $\mathcal{G}_\xi \leq (\sigma[\mathfrak{g}_{U,\xi}] + \sigma[\mathfrak{g}_{S,\xi}])^2$ is saturated. In this section, we discuss under which general conditions the bound given in Prop. 1 can be tight. We discover that tightness depends only on a mathematical property of the Hamiltonian H_ξ , explained below. Therefore, for all Hamiltonians belonging to such special class, \mathcal{G}_ξ can be readily computed in terms of the spectral gaps of the generators of U_t and S_ξ .

Let us summarize the steps that went into proving the bound of Prop. 1. First, we bounded the FI from above, in Eq. (19) (step 1). Next, we optimized over the initial preparation, which led to Eq. (23) (step 2). Finally, we optimized over the unitary control V by means of Lemma 1 (step 3). The last two steps were proper maximizations, so they can be made tight by implementing the optimal control V_{opt} and the optimal initial preparation $|\psi_{0,opt}\rangle$. The optimal control V_{opt} , which achieves the maximum in step 3, is obtained from the proof of Lemma 1:

$$V_{opt} = S_\xi^\dagger R_1^\dagger R_2, \quad (37)$$

where R_1 (resp., R_2) is the similarity transformation which diagonalizes $\mathfrak{g}_{S,\xi}$ (resp., $\mathfrak{g}_{U,\xi}$), with eigenvalues ordered decreasingly, i.e.

$$\begin{aligned} R_1 \mathfrak{g}_{S,\xi} R_1^\dagger &= \text{diag} [\lambda_1(\mathfrak{g}_{S,\xi}), \dots, \lambda_d(\mathfrak{g}_{S,\xi})], \\ R_2 \mathfrak{g}_{U,\xi} R_2^\dagger &= \text{diag} [\lambda_1(\mathfrak{g}_{U,\xi}), \dots, \lambda_d(\mathfrak{g}_{U,\xi})]. \end{aligned}$$

The optimal preparation $|\psi_{0,opt}\rangle$, which achieves the maximum in step 2, is related to the extremal eigenvectors of $\mathcal{U}_{opt}^\dagger \mathfrak{g}_{\mathcal{U}_{opt},\xi} \mathcal{U}_{opt}$, where $\mathcal{U}_{opt} := S_\xi V_{opt} U_t$ and $\mathfrak{g}_{\mathcal{U}_{opt},\xi}$ is its generator. Explicitly,

$$|\psi_{0,opt}\rangle = \frac{1}{\sqrt{2}} \mathcal{U}_{opt}^\dagger [|\lambda_1(\mathfrak{g}_{\mathcal{U}_{opt},\xi})\rangle + e^{i\varphi} |\lambda_d(\mathfrak{g}_{\mathcal{U}_{opt},\xi})\rangle], \quad (38)$$

where $\varphi \in \mathbb{R}$.

Tightness of inequality (35) is thus reduced to that of step 1, with the control and the initial preparation chosen according

to Eqs. (37) and (38), respectively. In turn, step 1 involves two majorizations. The first majorization is based on the Cauchy-Schwarz inequality of Eq. (18), which is saturated iff

$$\sqrt{\rho_{opt}} P_j \propto \sqrt{\rho_{opt}} L_{\rho_{opt},\xi} P_j, \quad \forall j \in \{0, \dots, d-1\}, \quad (39)$$

where $\rho_{opt} := \mathcal{U}_{opt} \rho_{0,opt} \mathcal{U}_{opt}^\dagger$, $L_{\rho_{opt},\xi}$ is its SLD and the proportionality constant may depend on j . Condition (39) is always satisfied thanks to the fact that the model is pure, i.e. $|\psi_{opt}\rangle := \mathcal{U}_{opt} |\psi_{0,opt}\rangle$, since then it reduces to the manifestly true relation

$$\langle \psi_{opt}|j\rangle |\psi_{opt}\rangle \langle j| \propto \langle \psi_{opt}| L_{\psi_{opt},\xi} |j\rangle |\psi_{opt}\rangle \langle j|. \quad (40)$$

The second majorization is based on the triangular inequality of Eq. (17). It is proven below that saturation occurs iff the unitary matrix S_ξ has *equioriented* extremal eigenvectors (two complex vectors v_1, v_2 are said to be equioriented, with respect to a given orthonormal basis $|b_j\rangle$, if $|\langle b_j|v_1\rangle| = |\langle b_j|v_2\rangle|, \forall j \in \{0, \dots, d-1\}$). For all Hamiltonians such that the matrix S_ξ has the previous property, inequality (35) becomes an equality. We collect our results in the following two propositions.

PROPOSITION 2. *The inequality given in Prop. 1 is an equality when the Hamiltonian H_ξ is such that the extremal eigenvectors of the generator $\mathfrak{g}_{S,\xi}$ of S_ξ are equioriented with respect to the computational basis.*

Proof. Most of the proof is contained in the discussion preceding Eq. (2). What is left to check is that the triangular inequality of Eq. (17) is saturated whenever $\mathfrak{g}_{S,\xi}$ has equioriented extremal eigenvectors. For Eq. (17) to be tight, it must be that, $\forall j \in \{0, \dots, d-1\}$,

$$\Im \text{tr} (\rho_{opt} L_{\rho_{opt},\xi} P_j) = 0, \quad (41)$$

which is also equivalent to

$$\Im [\langle j| L_{\psi_{opt},\xi} |\psi_{opt}\rangle \langle \psi_{opt}|j\rangle] = 0. \quad (42)$$

The SLD $L_{\psi_{opt},\xi}$ is given by

$$L_{\psi_{opt},\xi} = 2 |\partial_\xi \psi_{opt}\rangle \langle \psi_{opt}| + 2 |\psi_{opt}\rangle \langle \partial_\xi \psi_{opt}|, \quad (43)$$

which can be rewritten as

$$L_{\psi_{opt},\xi} |\psi_{opt}\rangle = 2i (\langle \psi_{opt}| \mathfrak{g}_{\mathcal{U}_{opt},\xi} |\psi_{opt}\rangle - \mathfrak{g}_{\mathcal{U}_{opt},\xi}) |\psi_{opt}\rangle. \quad (44)$$

Substituting this result in Eq. (42), one arrives at the condition

$$\langle \psi_{opt}| \mathfrak{g}_{\mathcal{U}_{opt},\xi} |\psi_{opt}\rangle |\langle j|\psi_{opt}\rangle|^2 = \Re[\langle j| \mathfrak{g}_{\mathcal{U}_{opt},\xi} |\psi_{opt}\rangle \langle \psi_{opt}|j\rangle] \quad (45)$$

or, using the explicit form of the optimal preparation given in Eq. (38),

$$\begin{aligned} 0 &= \left(|\langle j|\lambda_1(\mathfrak{g}_{\mathcal{U}_{opt},\xi})\rangle|^2 - |\langle j|\lambda_d(\mathfrak{g}_{\mathcal{U}_{opt},\xi})\rangle|^2 \right) \\ &\quad \times [\lambda_1(\mathfrak{g}_{\mathcal{U}_{opt},\xi}) - \lambda_d(\mathfrak{g}_{\mathcal{U}_{opt},\xi})]. \end{aligned} \quad (46)$$

The conclusion is that the extremal eigenvectors of $\mathfrak{g}_{\mathcal{U}_{opt},\xi}$

must be equioriented. To finish the proof, we have to show that $|\lambda_i(\mathfrak{g}_{U_{opt}, \xi})\rangle = |\lambda_i(\mathfrak{g}_S)\rangle$ for $i = 1, d$. This can be proven as follows. Note that

$$\mathfrak{g}_{U_{opt}, \xi} = \mathfrak{g}_S + R_1^\dagger R_2 \mathfrak{g}_{U, \xi} R_2^\dagger R_1 = R_1^\dagger D R_1, \quad (47)$$

where D is the diagonal matrix

$$D = \text{diag}[\lambda_1(\mathfrak{g}_S, \xi) + \lambda_1(\mathfrak{g}_{U, \xi}), \dots, \lambda_d(\mathfrak{g}_S, \xi) + \lambda_d(\mathfrak{g}_{U, \xi})].$$

Therefore, the extremal eigenvectors of $\mathfrak{g}_{U_{opt}, \xi}$ are given by $R_1^\dagger |1\rangle$ and $R_1^\dagger |d\rangle$. But, by definition of R_1 , these are also the extremal eigenvectors of \mathfrak{g}_S, ξ . \square

PROPOSITION 3. *If the conditions of Prop. 2 are satisfied, the strategy which saturates the bound (35) makes use of the optimal control $V_{opt} = S_\xi^\dagger R_1^\dagger R_2$ and the optimal initial preparation $|\psi_{0, opt}\rangle$, i.e.*

$$|\psi_{0, opt}\rangle = \frac{1}{\sqrt{2}} (S_\xi V_{opt} U_t)^\dagger [|\lambda_1(\mathfrak{g}_S, \xi)\rangle + e^{i\varphi} |\lambda_d(\mathfrak{g}_S, \xi)\rangle],$$

where $\varphi \in \mathbb{R}$ and R_1 (resp., R_2) is the similarity transformation which diagonalizes \mathfrak{g}_S, ξ (resp., $\mathfrak{g}_{U, \xi}$), with eigenvalues ordered decreasingly.

Proof. Follows immediately from Eq. (37) and (38), together with the fact that $\mathfrak{g}_{U_{opt}, \xi}$ and \mathfrak{g}_S, ξ have the same extremal eigenvectors. \square

The condition that the extremal eigenvectors of \mathfrak{g}_S, ξ be equioriented might appear restrictive, but actually it is often satisfied in practice (see also Sect. VII). In such cases, the LHS of Eq. (35) provides a simple expression for \mathcal{G}_ξ . The possible precision enhancement with respect to the optimal Braunstein-Caves measurement is then quantified by

$$\Delta = (\sigma[\mathfrak{g}_{U, \xi}] + \sigma[\mathfrak{g}_S, \xi])^2 - \sigma[\mathfrak{g}_{U, \xi}]^2. \quad (48)$$

VI. APPLICATION TO METROLOGY

In this section, we illustrate the relevance of our previous results to quantum metrology applications. The main point to address is how to perform a controlled energy measurement on a physical system. In principle, one is required to initialize the system in a reference state ρ_0 , to encode the parameter ξ , to apply a unitary control V and finally to measure the energy. The problem is that the Hamiltonian is not fully known and, as a result, neither is the POVM to be implemented.

When the Hamiltonian is fully known, a projective energy measurement can be performed by a suitable modification of the phase estimation algorithm [54–56]. However, such an approach is not useful for parameter estimation, since it requires to know the parameter beforehand. Let us also emphasize that, for a controlled energy measurement to be non-regular, it is crucial that the measurement projects onto the eigenstates of the *true* Hamiltonian H_ξ . Otherwise, the measurement is regular (and thus cannot outperform the optimal

Braunstein-Caves measurement). In conclusion, our aim is to design a measurement such that its statistics coincides (or at least approximates closely) that of a controlled energy measurement *for all* $\xi \in \Xi$ assuming no knowledge about the system's Hamiltonian.

Let us now explain how to construct such a measurement, referred to as a realistic controlled energy measurement. The central idea is to make use of the system's unitary evolution as a resource, by means of a quantum subroutine, named *universal controllization* and developed in [57, 58]. First, we describe a simplified version of a controlled energy measurement (see Fig. 2), which is actually based on an unrealistic assumption; then, we explain how to remove such assumption. The assumption is that the experimenter can implement the controlled time-evolution operator

$$C_{U_t} := |0\rangle\langle 0| \otimes \mathbb{I}_d + |1\rangle\langle 1| \otimes U_t, \quad (49)$$

acting on the enlarged Hilbert space $\mathbb{C}^2 \otimes \mathcal{H}$, where $\mathcal{H} = \mathbb{C}^d$ is the Hilbert space of the main system and $U_t = \exp(-itH_\xi)$ is the time-evolution operator. The assumption is unrealistic because C_{U_t} still depends on the true value of the parameter ξ , which is not known.

In order to implement this simplified version, let us introduce n control qubits, each with Hilbert space $\mathcal{H}_c = \mathbb{C}^2$; the total Hilbert space is now $\mathcal{H}_c^{\otimes n} \otimes \mathcal{H}$. Each control qubit is prepared in the ground state $|0\rangle$. Thus, the initial state of the system is $|0\dots 0\rangle\langle 0\dots 0| \otimes \rho_0$. Next, a Hadamard gate is applied to each control qubit, i.e. $|0\rangle \rightarrow H|0\rangle = (|0\rangle + |1\rangle)/\sqrt{2}$. Meanwhile, the parameter is encoded into $\rho_\xi = U_t \rho_0 U_t^\dagger$ and the unitary control V is applied. Therefore, the state of the total system up to this step is

$$\frac{1}{2^n} \sum_{x, y \in \{0, 1\}^{\times n}} |x_1 \dots x_n\rangle\langle y_1 \dots y_n| \otimes V \rho_\xi V^\dagger, \quad (50)$$

where x stands for the generic binary n -string $x_1 \dots x_n$.

Given any unitary U acting on \mathcal{H} , the superoperator C_U is defined as follows,

$$C_U[\rho] := C_U \rho C_U^\dagger. \quad (51)$$

For $l = 1, \dots, n$, the n superoperators $C_{U_\tau^{2^{l-1}}}$ are applied between the l^{th} control qubit and the main system (τ is a free parameter giving the timescale of the measurement process). Notice that, when $C_{U_\tau^{2^{l-1}}}$ is applied to $\rho_l := |x_l\rangle\langle y_l| \otimes V \rho_\xi V^\dagger$, one obtains

$$C_{U_\tau^{2^{l-1}}}[\rho_l] = |x_l\rangle\langle y_l| \otimes U_\tau^{x_l 2^{l-1}} V \rho_\xi V^\dagger (U_\tau^\dagger)^{y_l 2^{l-1}}. \quad (52)$$

Denoting by $X = x_1 + 2 \cdot x_2 + \dots + 2^{n-1} \cdot x_n$ the decimal representation of the binary string x , the resulting total state is

$$\frac{1}{2^n} \sum_{X=0}^{2^n-1} \sum_{Y=0}^{2^n-1} |x\rangle\langle y| \otimes U_\tau^X V \rho_\xi V^\dagger (U_\tau^\dagger)^Y. \quad (53)$$

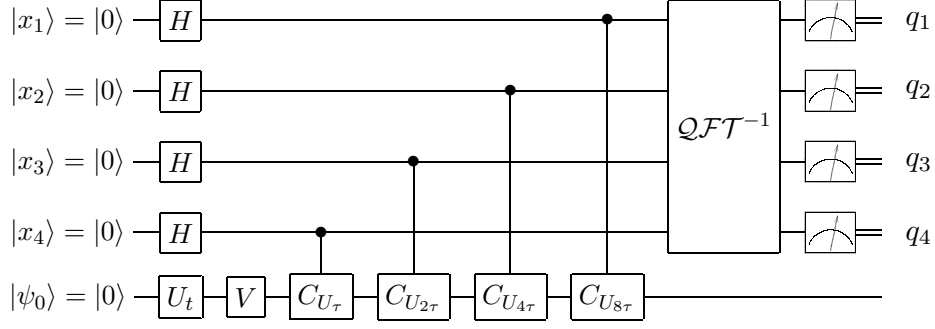


FIG. 2. Circuit diagram of a simplified realistic controlled energy measurement with $n = 4$ control qubits. A realistic controlled energy measurement replaces each application of C_{U_τ} by m repeated applications of $\Gamma_{U_\tau/m}$, defined in Eq. (63).

Let us expand $V\rho_\xi V^\dagger$ on the energy eigenbasis, i.e.

$$V\rho_\xi V^\dagger = \sum_{j=0}^{d-1} \sum_{k=0}^{d-1} c_{jk} |E_{j,\xi}\rangle \langle E_{k,\xi}|. \quad (54)$$

Eq. (53) then becomes

$$\frac{1}{2^n} \sum_{j,k=0}^{d-1} \sum_{X,Y=0}^{2^n-1} c_{jk} e^{-i\tau(XE_{j,\xi} - YE_{k,\xi})} |x\rangle \langle y| \otimes |E_{j,\xi}\rangle \langle E_{k,\xi}|. \quad (55)$$

The next step is to apply an inverse quantum Fourier transform QFT^{-1} on the n control qubits. By definition, QFT^{-1} acts as follows on the computational basis of $\mathcal{H}_c^{\otimes n}$:

$$QFT^{-1} |x\rangle = \frac{1}{2^{n/2}} \sum_{Q=0}^{2^n-1} e^{-\frac{2\pi i x Q}{2^n}} |q\rangle. \quad (56)$$

After application of QFT^{-1} , the total state of the system is

$$\frac{1}{2^{2n}} \sum_{j,k=0}^{d-1} \sum_{X,Y=0}^{2^n-1} \sum_{Q,P=0}^{2^n-1} \tilde{c}_{jk} |q\rangle \langle p| \otimes |E_{j,\xi}\rangle \langle E_{k,\xi}|. \quad (57)$$

where

$$\tilde{c}_{jk} = c_{jk} e^{-iX(\tau E_{j,\xi} + \frac{2\pi Q}{2^n})} e^{iY(\tau E_{k,\xi} + \frac{2\pi P}{2^n})}. \quad (58)$$

The last step is to perform a measurement of the n control qubits in the computational basis. The probability $p_{q,\xi}$ of obtaining as outcome the binary string q is

$$p_{q,\xi} = \frac{1}{2^{2n}} \sum_{j=0}^{d-1} \sum_{X,Y=0}^{2^n-1} p_{E_{j,\xi}} e^{-i(X-Y)\alpha_{j,Q}}, \quad (59)$$

where

$$\alpha_{j,Q} := \tau E_{j,\xi} + \frac{2\pi Q}{2^n}, \quad p_{E_{j,\xi}} = \langle E_{j,\xi} | V\rho_\xi V^\dagger | E_{j,\xi} \rangle. \quad (60)$$

By algebraic manipulation, Eq. (59) can also be written as

$$p_{q,\xi} = \sum_{j=0}^{d-1} p_{E_{j,\xi}} \left(\frac{1}{2^n} \frac{\sin(2^n \alpha_{j,Q}/2)}{\sin(\alpha_{j,Q}/2)} \right)^2. \quad (61)$$

In the limit $n \rightarrow \infty$, the probability distribution $p_{q,\xi}$ converges to the probability distribution $p_{E_{j,\xi}}$ corresponding to a controlled energy measurement $\mathcal{M}_{V,\xi}$.

We now explain how to implement the controlled time-evolution operator without full knowledge of the Hamiltonian. For a more detailed treatment, we refer the reader to Ref. [57]. For notational simplicity consider the case $l = 1$, so that the problem is to approximate the action of C_{U_τ} on the state $\rho_1 = |x_1\rangle \langle y_1| \otimes V\rho_\xi V^\dagger$. Since C_{U_τ} is not actually available, it is replaced by m applications of the superoperator $\Gamma_{U_\tau/m}$, constructed as follows. First of all, we introduce an ancilla having the same dimension as the main system, so that the total Hilbert space is $\mathcal{H}_c^{\otimes n} \otimes \mathcal{H} \otimes \mathcal{H}_a$, with $\mathcal{H}_a = \mathbb{C}^d$. The ancilla is prepared in the maximally mixed state. Therefore, the state of the first control qubit, the main system and the ancilla before application of C_{U_τ} is $\rho'_1 = |x_1\rangle \langle y_1| \otimes V\rho_\xi V^\dagger \otimes \mathbb{I}_d/d$. Let us define the following quantum operation,

$$W_{U_\tau} := C_{SWAP}(\mathbb{I}_2 \otimes U_\tau \otimes \mathbb{I}_d) C_{SWAP}, \quad (62)$$

where C_{SWAP} is the controlled-SWAP gate acting as follows on $\mathcal{H}_c \otimes \mathcal{H} \otimes \mathcal{H}_a$: $C_{SWAP}(|0\rangle \otimes |\psi\rangle \otimes |\phi\rangle) = |0\rangle \otimes |\phi\rangle \otimes |\psi\rangle$ and $C_{SWAP}(|1\rangle \otimes |\psi\rangle \otimes |\phi\rangle) = |0\rangle \otimes |\psi\rangle \otimes |\phi\rangle$. The key remark is that implementation of W_{U_τ} does not require knowledge of the Hamiltonian, but makes use instead of the uncontrolled version of the time-evolution operator U_τ (see also Fig. 3).

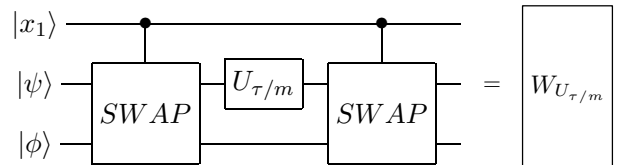


FIG. 3. Circuit diagram of $W_{U_\tau/m}$.

We now subdivide τ into m subintervals of length τ/m . During each subinterval, $W_{U_{\tau/m}}$ is applied; then the ancilla is discarded; finally, the ancilla is refreshed to its initial state. For instance, after the first interval, one obtains $\Gamma_{U_{\tau/m}}[\rho_1] \otimes \mathbb{I}_d/d$, where

$$\Gamma_{U_{\tau/m}}[\rho_1] := \text{tr}_{\mathcal{H}_a} \left(W_{U_{\tau/m}} \rho'_1 W_{U_{\tau/m}}^\dagger \right). \quad (63)$$

A simple computation reveals that

$$\Gamma_{U_{\tau/m}}[\rho_1] = \frac{1}{d} \text{tr} \left(U_{\tau/m}^{y_1 - x_1} \right) \mathcal{C}_{U_{\tau/m}}[\rho_1]. \quad (64)$$

For future convenience, we write

$$\frac{1}{d} \text{tr} \left(U_{\tau/m} \right) = a_{\tau/m} e^{i\phi_{\tau/m}}, \quad (65)$$

where $a_{\tau/m} \in \mathbb{R}^+$ and $\phi_{\tau/m} \in \mathbb{R}$. Note that, since $x_1 - y_1 \in \{-1, 0, 1\}$, one can write

$$\Gamma_{U_{\tau/m}}^m[\rho_1] = a_{\tau/m}^{|x_1 - y_1| m} e^{i(y_1 - x_1)m\phi_{\tau/m}} \mathcal{C}_{U_{\tau/m}}[\rho_1]. \quad (66)$$

Universal controllization basically replaces $\mathcal{C}_{U_{\tau/m}}$ with $\Gamma_{U_{\tau/m}}^m$. In the limit $m \rightarrow \infty$, it can be proven that the error

$$\epsilon_m := \left[\text{tr} \left(U_{\tau/m} \right) / d \right]^m - 1 \quad (67)$$

tends to zero. A realistic controlled energy measurement is thus obtained by substituting each application of $\mathcal{C}_{U_{\tau/m}^{2^{l-1}}}$ by $2^{l-1}m$ applications of $\Gamma_{U_{\tau/m}}$. For instance, instead of Eq. (53), one would have

$$\frac{1}{2^n} \sum_{X,Y=0}^{2^n-1} \pi_{X,Y} e^{i(Y-X)m\phi_{\tau/m}} |x\rangle\langle y| \otimes U_{\tau}^X V \rho_{\xi} V^\dagger (U_{\tau}^\dagger)^Y, \quad (68)$$

where we defined

$$\pi_{X,Y} := \prod_{l=1}^n a_{\tau/m}^{|x_l - y_l| 2^{l-1} m}. \quad (69)$$

After applying the inverse quantum Fourier transform and measuring in the computational basis, the probability of obtaining the outcome $q \in \{0, 1\}^{\times n}$ is

$$p_{q,\xi} = \frac{1}{2^{2n}} \sum_{j=0}^{d-1} p_{E_j,\xi} \sum_{X,Y=0}^{2^n-1} \pi_{X,Y} e^{i(Y-X)\beta_{j,Q}}, \quad (70)$$

with

$$\beta_{j,Q} := \alpha_{j,Q} + m\phi_{\tau/m}. \quad (71)$$

Eq. (70) can be further expanded by rewriting it as follows,

$$\begin{aligned} p_{q,\xi} &= \frac{1}{2^{2n}} \sum_{j=0}^{d-1} p_{E_j,\xi} \prod_{l=1}^n \sum_{u,v=0}^1 a_{\tau/m}^{|u-v|2^{l-1}m} e^{i(v-u)2^{l-1}\beta_{j,Q}} \\ &= \frac{1}{2^n} \sum_{j=0}^{d-1} p_{E_j,\xi} \prod_{l=1}^n \left[1 + a_{\tau/m}^{2^{l-1}m} \cos(2^{l-1}\beta_{j,Q}) \right] \end{aligned} \quad (72)$$

If $m \rightarrow \infty$, then $\phi_{\tau/m} \rightarrow 0$ and $a_{\tau/m} \rightarrow 1$, so that Eq. (72) converges to Eq. (61). Therefore, a realistic controlled energy measurement allows to approximate to any desired precision a controlled energy measurement $\mathcal{M}_{V,\xi}$, without requiring any a priori knowledge about the parameter ξ . The result is asymptotic, in the sense that the previous statement holds when both, the number of control qubits n and the number of subintervals m , go to infinity. In the next section, we discuss in detail a prototypical example and find that, even for small values of n and m , a controlled energy measurement can be well approximated, and thus a precision enhancement is possible compared to the optimal Braunstein-Caves measurement.

VII. EXAMPLES: QUANTUM MAGNETOMETRY

A. Qubit magnetometry: estimating the direction of a magnetic field

The problem is to estimate the polar angular direction ξ of an external magnetic field of known magnitude B by use of a qubit probe, with Hilbert space $\mathcal{H} = \mathbb{C}^2$ and Hamiltonian $H_\xi = \omega(\cos \xi \sigma_z + \sin \xi \sigma_x)$ (the energy splitting ω is proportional to B , thus it is assumed to be known). In the first part of this section, we compare the family of regular measurements \mathcal{R} with the non-regular family \mathcal{E} of controlled energy measurements. Next, we analyze the problem in a more physical setting, by evaluating the performance achievable via realistic controlled energy measurements.

The probe is initialized at time $t = 0$ in the state $|\psi_0\rangle = |0\rangle$. The parameter is encoded unitarily for a time t , leading to $|\psi_\xi\rangle = U_t |\psi_0\rangle$, with $U_t := \exp(-iH_\xi t)$. Let us suppose first that only regular measurements are allowed. Then, the best achievable performance is given by the QFI,

$$\mathcal{F}_\xi^{(Q)}(|\psi_\xi\rangle) = 4 \sin^2(\omega t) - \sin^2(2\omega t) \sin^2 \xi. \quad (73)$$

Optimizing also over the initial preparation $|\psi_0\rangle$, one arrives at the CQFI $\mathcal{F}_\xi^{(Q,C)} = 4 \sin^2(\omega t)$.

Suppose instead that the measurement is taken from the family of controlled energy measurements. Then, the best achievable precision is given by the information quantity \mathcal{G}_ξ of Eq. (14). Let us compute the matrix S_ξ , built from the eigenvectors of H_ξ , and its generator $\mathfrak{g}_{S,\xi}$:

$$S_\xi = \begin{pmatrix} -\text{sgn} \left[\cos \left(\frac{\xi}{2} \right) \right] \sin \left(\frac{\xi}{2} \right) & \text{sgn} \left[\cos \left(\frac{\xi}{2} \right) \right] \cos \left(\frac{\xi}{2} \right) \\ \text{sgn} \left[\sin \left(\frac{\xi}{2} \right) \right] \cos \left(\frac{\xi}{2} \right) & \text{sgn} \left[\sin \left(\frac{\xi}{2} \right) \right] \sin \left(\frac{\xi}{2} \right) \end{pmatrix},$$

$$\mathfrak{g}_{S,\xi} = \begin{pmatrix} 0 & -\frac{i}{2} \operatorname{sgn}(\sin \xi) \\ \frac{i}{2} \operatorname{sgn}(\sin \xi) & 0 \end{pmatrix},$$

where $\operatorname{sgn}(x) = |x|/x$. The extremal eigenvectors of $\mathfrak{g}_{S,\xi}$ are

$$|\lambda_1(\mathfrak{g}_{S,\xi})\rangle = \frac{1}{\sqrt{2}} (-i, 1)^t, \quad |\lambda_2(\mathfrak{g}_{S,\xi})\rangle = \frac{1}{\sqrt{2}} (i, 1)^t.$$

Since they are equioriented, by Prop. (2) \mathcal{G}_ξ can be computed as

$$\mathcal{G}_\xi = (\sigma[\mathfrak{g}_{U,\xi}] + \sigma[\mathfrak{g}_{S,\xi}])^2. \quad (74)$$

The explicit expressions for U_t and its generator are

$$U_t = \begin{pmatrix} A & B \\ B & A^* \end{pmatrix}, \quad \mathfrak{g}_{U,\xi} = \begin{pmatrix} -C & D \\ D^* & C \end{pmatrix}$$

where

$$\begin{aligned} A &= \cos \omega t - i \cos \xi \sin \omega t \\ B &= -i \sin \xi \sin \omega t \\ C &= \frac{1}{2} \sin \xi \sin 2\omega \\ D &= (\cos \xi \cos \omega t - i \sin \omega t) \sin \omega t. \end{aligned} \quad (75)$$

After diagonalizing $\mathfrak{g}_{U,\xi}$ and $\mathfrak{g}_{S,\xi}$, one can compute \mathcal{G}_ξ via Eq. (74), which gives

$$\mathcal{G}_\xi = \mathcal{F}_\xi^{(Q,C)} + 4|\sin(\omega t)| + 1. \quad (76)$$

As $\mathcal{G}_\xi > \mathcal{F}_\xi^{(Q,C)}$, the optimal Braunstein-Caves measurement is outperformed. A comparison is shown in Fig. 4.

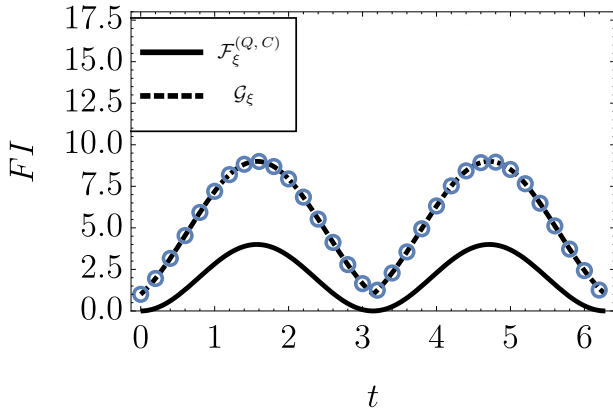


FIG. 4. Comparison between the optimal Braunstein-Caves measurement and the optimal controlled energy measurement, for the estimation of the polar angular direction of a magnetic field via a qubit probe. The solid line is the QFI, while the dashed line corresponds to \mathcal{G}_ξ , computed by Eq. (76). The circular marks denote \mathcal{G}_ξ , computed by numerical optimization, from its definition (14), thus confirming that the bound given in Prop. 1 is saturated.

Finally, we study numerically the case when the measurement is a realistic controlled energy measurement. This re-

quires to introduce n ancillary qubits and implement the quantum algorithm described in Sect. VI. In particular, universal controllization is needed to approximate the action of the controlled time-evolution operator \mathcal{C}_{U_τ} , by subdividing τ into m subintervals and applying the superoperator $\Gamma_{U_\tau/m}$ of Eq. (63) in each subinterval. In the limit $n, m \rightarrow \infty$, one performs the corresponding controlled energy measurement exactly (and thus can achieve \mathcal{G}_ξ of Eq. (74)). The two panels of Fig. 5 show the performance of the optimal realistic controlled energy measurement, for different values of n and m . Reasonably small values of the two parameters (e.g. $n = 6$ and $m = 3$) are enough to come close to the ultimate bound \mathcal{G}_ξ of Eq. (76).

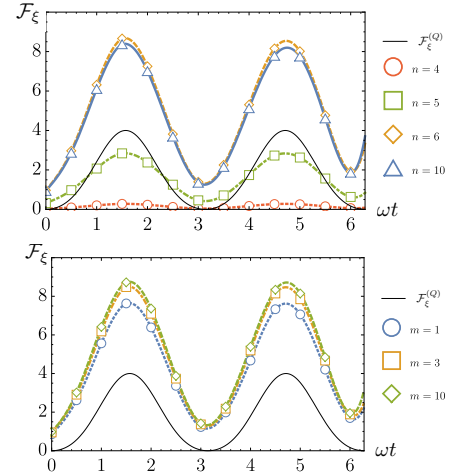


FIG. 5. *Upper panel*: FI of the best-performing realistic controlled energy measurement, for different values of n and fixed $m = 5$. Each marker represents the maximum FI, taken over the family of realistic controlled energy measurements for given n, m, τ and interrogation time t . The curves are obtained by interpolation. The thin solid curve corresponds to the QFI of Eq. (73). Notice that the optimal Braunstein-Caves measurement is outperformed already for $n = 6$. *Lower panel*: FI of the best-performing realistic controlled energy measurement, for different values of m and fixed $n = 6$. Both plots are obtained for $\omega = 1$ and $\tau = 0.1$ (in the natural units of the problem), while the true value of the parameter is taken to be $\xi = \pi/4$.

B. Qubit magnetometry: estimating one component of a magnetic field

Here the task is to estimate one component of an external magnetic field along a given direction (which, without loss of generality, is taken to be parallel to the x axis) via a qubit probe. The Hamiltonian is $H_\xi = -\omega\sigma_z + \xi\sigma_x$, with eigenvalues $\pm\Omega_\xi$, where $\Omega_\xi := \sqrt{\omega^2 + \xi^2}$. As before, one has to compute the relevant matrices U_t, S_ξ , and their corresponding generators. Concerning U_t and $\mathfrak{g}_{U,\xi}$, we have

$$U_t = \begin{pmatrix} A & B \\ B & A^* \end{pmatrix}, \quad \mathfrak{g}_{U,\xi} = \begin{pmatrix} -C & D \\ D^* & C \end{pmatrix}$$

where

$$\begin{aligned} A &= \cos(\Omega_\xi t) + \frac{i\omega \sin(\Omega_\xi t)}{\Omega_\xi} \\ B &= -\frac{i\xi \sin(\Omega_\xi t)}{\Omega_\xi} \\ C &= -\frac{\omega\xi [\sin(2\Omega_\xi t) - 2\Omega_\xi t]}{2\Omega_\xi^3} \\ D &= \frac{\sin(2\Omega_\xi t)\omega^2 - i\Omega_\xi \cos(2\Omega_\xi t)\omega + \Omega_\xi (2t\xi^2 + i\omega)}{2\Omega_\xi^3}. \end{aligned} \quad (77)$$

S_ξ and its generator $\mathfrak{g}_{S, \xi}$ are instead given by

$$S_\xi = \frac{1}{\sqrt{2\Omega_\xi}} \begin{pmatrix} -\frac{\omega+\Omega_\xi}{\sqrt{\Omega_\xi+\omega}} & \frac{\xi}{\sqrt{\Omega_\xi+\omega}} \\ \frac{\xi}{\sqrt{\Omega_\xi+\omega}} & \frac{\xi}{\sqrt{\Omega_\xi-\omega}} \end{pmatrix}, \quad (78)$$

$$\mathfrak{g}_{S, \xi} = \begin{pmatrix} 0 & \frac{i\omega}{2\xi^2} \\ -\frac{i\omega}{2\xi^2} & 0 \end{pmatrix}. \quad (79)$$

The CQFI is found by diagonalizing $\mathfrak{g}_{U, \xi}$, i.e.

$$\mathcal{F}_\xi^{(Q, C)} = \frac{2}{\Omega_\xi^4} [2\Omega_\xi^2 t^2 \xi^2 - \omega^2 \cos(2\Omega_\xi t) + \omega^2]. \quad (80)$$

Since the eigenvectors of $\mathfrak{g}_{S, \xi}$ are equioriented, \mathcal{G}_ξ can be computed directly,

$$\mathcal{G}_\xi = \left(\frac{\omega}{\Omega_\xi^2} + \frac{\sqrt{2[2\Omega_\xi^2 t^2 \xi^2 - \omega^2 \cos(2\Omega_\xi t) + \omega^2]}}{\Omega_\xi^2} \right)^2. \quad (81)$$

A comparison similar to that of Fig. 4 is shown in Fig. 6.

C. NV-center magnetometry

As a last example, we study the problem of estimating a weak magnetic field via an NV-center in diamond. An NV center consists of a nitrogen atom (N) inside a diamond crystal lattice, having a vacancy (V) in one of its neighboring sites. Two different kinds of the defect are known: the neutral state NV_0 and the negatively-charged state NV_- , which is the most interesting for metrological applications. The NV_- form provides a spin triplet state which can be initialized, manipulated with long coherence time and readout by purely optical means. The reader is referred to the review [59] for more details.

Neglecting the interactions with the surrounding nuclear spins, and setting $\hbar = 1$, the Hamiltonian H_{NV} for the triplet state of the NV center can be written in the form

$$H_{NV} = \mu \mathbf{B} \cdot \mathbf{S} + D S_z^2 + E (S_x^2 - S_y^2), \quad (82)$$

where \mathbf{B} is the applied magnetic field and $\mathbf{S} = (S_x, S_y, S_z)$

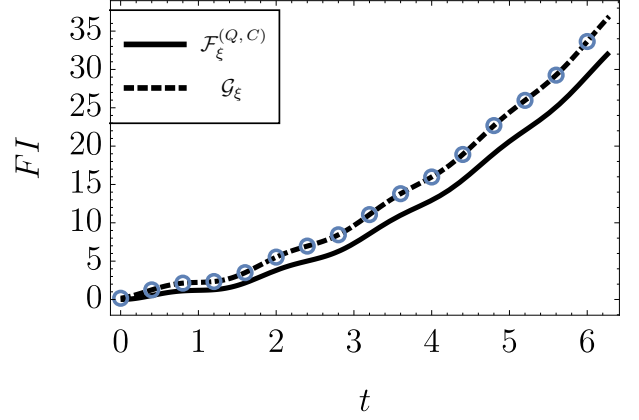


FIG. 6. Comparison between the optimal Braunstein-Caves measurement and the optimal controlled energy measurement, for the estimation of one component of a magnetic field via a qubit probe. The solid line is the CQFI, while the dashed line corresponds to \mathcal{G}_ξ . The circular marks denote \mathcal{G}_ξ , computed by numerical optimization, from its definition (14), thus confirming that the bound given in Prop. 1 is saturated.

is a vector made up by the three spin 1 matrices

$$\begin{aligned} S_x &= \sqrt{2} \begin{pmatrix} 0 & 1 & 0 \\ 1 & 0 & 1 \\ 0 & 1 & 0 \end{pmatrix}, \quad S_y = \sqrt{2}i \begin{pmatrix} 0 & -1 & 0 \\ 1 & 0 & -1 \\ 0 & 1 & 0 \end{pmatrix}, \\ S_z &= 2 \begin{pmatrix} 1 & 0 & 0 \\ 0 & 0 & 0 \\ 0 & 0 & -1 \end{pmatrix}. \end{aligned} \quad (83)$$

Moreover, $D \approx \pi \times 1.44$ GHz, $E \approx \pi \times 50$ kHz and μ is the Bohr magneton. We work in the weak magnetic field regime, where the transversal components B_x and B_y can be neglected compared to the component B_z aligned along the NV-center defect axis.

The task is to estimate the field component B_z , which from now on we denote conventionally by ξ . The CQFI is found to be

$$\mathcal{F}_\xi^{(Q, C)} = \frac{8\mu^2 [2\xi^2 \mu^2 t^2 \chi^2 + E^2 - E^2 \cos(4\chi t)]}{\chi^4}, \quad (84)$$

where $\chi := \sqrt{\xi^2 \mu^2 + 4E^2}$, while \mathcal{G}_ξ is given by

$$\mathcal{G}_\xi = \left(\frac{2E\mu}{\chi^2} + 2\sqrt{2}\mu \frac{\sqrt{2\xi^2 \mu^2 t^2 \chi^2 + E^2 - E^2 \cos(4\chi t)}}{\chi^2} \right)^2. \quad (85)$$

A comparison is shown in Fig. 7.

VIII. CONCLUSIONS

In this paper, the main focus has been on a class of *non-regular* quantum measurements, referred to as controlled en-

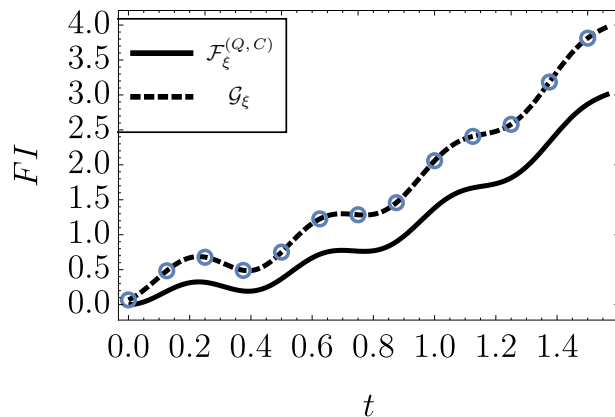


FIG. 7. Comparison between the optimal Braunstein–Caves measurement and the optimal controlled energy measurement for the estimation of the magnitude of a weak magnetic field via a NV-center in diamond. The solid line is the CQFI, while the dashed line corresponds to \mathcal{G}_ξ . The circular marks denote \mathcal{G}_ξ , computed by numerical optimization, from its definition (14), thus confirming that the bound given in Prop. 1 is saturated.

ergy measurements, that are naturally available in the estimation of a general Hamiltonian parameter. We have introduced the information quantity \mathcal{G}_ξ , which gives the best achievable precision over such a class, and provided an upper-bound to

it, that can often be saturated in practice. We have also discussed a realistic implementation of controlled energy measurements, which makes use of the phase estimation algorithm and a quantum subroutine known as universal controllization. Finally, we have applied our results to a few prototypical estimation problems and found a precision enhancement with respect to the optimal Braunstein–Caves measurement.

The difficulty, as a matter of principle, of encoding the (unknown) parameter into the measurement apparatus is solved by making use of the time-evolution generated by the system’s Hamiltonian as a resource. In this way, the POVM elements formally acquire an intrinsic dependence on the parameter, which in turn makes an analysis based only on the quantum Fisher information insufficient to capture the ultimate precision bounds. Our results thus show that for Hamiltonian parameters that are not just phase parameters, it is possible to overcome the Cramér–Rao bound by feasible detection schemes, opening new avenues to the precise estimation of physical parameters at the quantum frontier.

ACKNOWLEDGMENTS

This work has been supported by JSPS through FY2017 program (grant S17118) and by SERB through the VAJRA award (grant VJR/2017/000011). The authors thank M. A. C. Rossi, F. Albarelli, T. Giani, and G. Guarnieri for discussion in the early stages of this work.

-
- [1] G. Casella and R. L. Berger, *Statistical inference*, Vol. 2 (Duxbury Pacific Grove, CA, 2002).
 - [2] H. L. Van Trees and K. L. Bell, *Detection estimation and modulation theory, pt. I* (Wiley, 2013).
 - [3] S. M. Kay, *Fundamentals of statistical signal processing* (Prentice Hall PTR, 1993).
 - [4] E. L. Lehmann and G. Casella, *Theory of point estimation* (Springer Science & Business Media, 2006).
 - [5] C. W. Helstrom, *Quantum detection and estimation theory* (Academic press, 1976).
 - [6] A. S. Holevo, *Probabilistic and statistical aspects of quantum theory*, Vol. 1 (Springer Science & Business Media, 2011).
 - [7] C. M. Caves, *Phys. Rev. D* **23**, 1693 (1981).
 - [8] G. M. D’Ariano, P. Lo Presti, and M. G. A. Paris, *Phys. Rev. Lett.* **87**, 270404 (2001).
 - [9] V. Giovannetti, S. Lloyd, and L. Maccone, *Phys. Rev. Lett.* **96**, 010401 (2006).
 - [10] V. Giovannetti, S. Lloyd, and L. Maccone, *Nat. Photonics* **5**, 222 (2011).
 - [11] R. Demkowicz-Dobrzański, J. Kołodyński, and M. Guţă, *Nat. Commun.* **3**, 1063 (2012).
 - [12] B. Escher, R. de Matos Filho, and L. Davidovich, *Nat. Phys.* **7**, 406 (2011).
 - [13] M. Tsang, *New J. Phys.* **15**, 073005 (2013).
 - [14] A. Fujiwara and H. Nagaoka, *Phys. Lett. A* **201**, 119 (1995).
 - [15] V. Giovannetti, S. Lloyd, and L. Maccone, *Science* **306**, 1330 (2004).
 - [16] G. Tóth and I. Apellaniz, *J. Phys. A* **47**, 424006 (2014).
 - [17] M. G. Paris, *Int. J. Quantum Inf.* **7**, 125 (2009).
 - [18] M. Hayashi, *Asymptotic theory of quantum statistical inference: selected papers* (World Scientific, 2005).
 - [19] S. Amari and H. Nagaoka, *Methods of information geometry*, Vol. 191 (American Mathematical Soc., 2007).
 - [20] O. E. Barndorff-Nielsen, R. D. Gill, and P. E. Jupp, *J. Royal Stat. Soc. Series B Stat. Methodol.* **65**, 775 (2003).
 - [21] S. F. Huelga, C. Macchiavello, T. Pellizzari, A. K. Ekert, M. B. Plenio, and J. I. Cirac, *Phys. Rev. Lett.* **79**, 3865 (1997).
 - [22] J. J. Bollinger, W. M. Itano, D. J. Wineland, and D. Heinzen, *Phys. Rev. A* **54**, R4649 (1996).
 - [23] J. P. Dowling, *Phys. Rev. A* **57**, 4736 (1998).
 - [24] U. Dorner, R. Demkowicz-Dobrzański, B. Smith, J. Lundeen, W. Wasilewski, K. Banaszek, and I. Walmsley, *Phys. Rev. Lett.* **102**, 040403 (2009).
 - [25] P. M. Anisimov, G. M. Raterman, A. Chiruvelli, W. N. Plick, S. D. Huver, H. Lee, and J. P. Dowling, *Phys. Rev. Lett.* **104**, 103602 (2010).
 - [26] D. Brivio, S. Cialdi, S. Vezzoli, B. T. Gebrehiwot, M. G. Genoni, S. Olivares, and M. G. A. Paris, *Phys. Rev. A* **81**, 012305 (2010).
 - [27] J. Joo, W. J. Munro, and T. P. Spiller, *Phys. Rev. Lett.* **107**, 083601 (2011).
 - [28] M. G. Genoni, S. Olivares, and M. G. Paris, *Phys. Rev. Lett.* **106**, 153603 (2011).
 - [29] H. Yonezawa, D. Nakane, T. A. Wheatley, K. Iwasawa, S. Takeda, H. Arao, K. Ohki, K. Tsumura, D. W. Berry, and T. C. Ralph, *Science* **337**, 1514 (2012).
 - [30] P. Kok, S. L. Braunstein, and J. P. Dowling, *J. Opt. B Quantum Semiclassical Opt.* **6**, S811 (2004).

- [31] L. Pezzé and A. Smerzi, Phys. Rev. Lett. **102**, 100401 (2009).
- [32] D. C. Brody and E.-M. Graefe, Entropy **15**, 3361 (2013).
- [33] S. Pang and T. A. Brun, Phys. Rev. A **90**, 022117 (2014).
- [34] L. Seveso, M. A. Rossi, and M. G. Paris, Phys. Rev. A **95**, 012111 (2017).
- [35] J. M. E. Fraïsse and D. Braun, Phys. Rev. A **95**, 062342 (2017).
- [36] H. Cramér, *Mathematical Methods of Statistics (PMS-9)*, Vol. 9 (Princeton university press, 2016).
- [37] C. R. Rao, in *Breakthroughs in statistics* (Springer, 1992) pp. 235–247.
- [38] R. A. Fisher, in *Mathematical Proceedings of the Cambridge Philosophical Society*, Vol. 22 (Cambridge University Press, 1925) pp. 700–725.
- [39] S. L. Braunstein and C. M. Caves, Phys. Rev. Lett. **72**, 3439 (1994).
- [40] Some caveats are necessary in order to clarify the previous proposition. If the optimal measurement depends on the true value of the parameter, an adaptive procedure is needed [60]. Moreover, if no unbiased efficient estimator exists, the Cramér-Rao bound can be saturated only in the asymptotic limit $N \rightarrow \infty$, by resorting to an asymptotically efficient estimator [52].
- [41] O. Barndorff-Nielsen and R. Gill, J. Phys. A **33**, 4481 (2000).
- [42] R. L. Smith, Biometrika **72**, 67 (1985).
- [43] H. Morimoto and M. Sibuya, Sankhyā: Indian J. Stat. Ser. A, **15** (1967).
- [44] M. Akahira, Rep. Stat. Appl. Res. Union Jpn. Sci. Eng. **22**, 8 (1975).
- [45] M. Akahira, Rep. Stat. Appl. Res. Union Jpn. Sci. Eng. **22**, 3 (1975).
- [46] M. Woodroffe, Ann. Math. Stat. **43**, 113 (1972).
- [47] T. Polfeldt, Ann. Math. Stat. **41**, 667 (1970).
- [48] M. Akahira and K. Takeuchi, *Non-regular statistical estimation*, Vol. 107 (Springer Science & Business Media, 2012).
- [49] S. L. Braunstein, C. M. Caves, and G. J. Milburn, arXiv preprint quant-ph/9507004 (1995).
- [50] D. Petz, Linear Algebra Appl. **244**, 81 (1996).
- [51] C. Helstrom, IEEE Trans. Inf. Theory **14**, 234 (1968).
- [52] A. Fujiwara, J. Phys. A **39**, 12489 (2006).
- [53] T. Popoviciu, Mathematica **9**, 129 (1935).
- [54] K. Temme, T. J. Osborne, K. G. Vollbrecht, D. Poulin, and F. Verstraete, Nature **471**, 87 (2011).
- [55] A. Riera, C. Gogolin, and J. Eisert, Phys. Rev. Lett. **108**, 080402 (2012).
- [56] A. Y. Kitaev, Electr. Coll. Comp. Compl. **TR96**, 3 (1996).
- [57] S. Nakayama, A. Soeda, and M. Murao, Phys. Rev. Lett. **114**, 190501 (2015).
- [58] Y. Matsuzaki, S. Nakayama, A. Soeda, S. Saito, and M. Murao, Phys. Rev. A **95**, 062106 (2017).
- [59] L. Rondin, J. Tetienne, T. Hingant, J. Roch, P. Maletinsky, and V. Jacques, Rep. Prog. Phys. **77**, 056503 (2014).
- [60] H. Nagaoka, in *Proc. Int. Symp. on Inform. Theory*, Vol. 198 (1988) pp. 577–82.